Far-infrared vibrational properties of tetragonal C_{60} polymer

Z.-T. Zhu
Department of Chemistry, State University of New York at Binghamton, Binghamton, New York 13902

J. L. Musfeldt
Department of Chemistry, University of Tennessee, Knoxville, Tennessee 37996

K. Kamarás
Research Institute for Solid State Physics and Optics, Hungarian Academy of Sciences, H-1525 Budapest, Hungary

G. B. Adams and J. B. Page
Department of Physics and Astronomy, Arizona State University, Tempe, Arizona 85287

V. A. Davydov, L. S. Kashevarova, and A. V. Rakhmanina
Institute for High Pressure Physics of the Russian Academy of Sciences, 142092, Troitsk, Moscow Region, Russian Federation
(Received 27 July 2001; published 7 February 2002)

We report high-resolution far-infrared transmittance measurements and quantum-molecular-dynamics calculations of the two-dimensional tetragonal (*T*) high-temperature/high-pressure C_{60} polymer, as a complement to our previous work on the C_{60} dimer, and the one-dimensional orthorhombic (*O*) and two-dimensional rhombohedral (*R*) C_{60} polymers [V. C. Long *et al.*, Phys. Rev. B **61**, 13 191 (2000)]. The spectral features are assigned as intramolecular modes according to our quantum-molecular-dynamics calculations. In addition, we determine the I_h C_{60} parent symmetry of each polymer vibrational mode by expanding the calculated polymer eigenvectors in terms of our calculated eigenvectors for I_h C_{60}. We find that many of the *T*-polymer vibrational modes are derived from more than one I_h C_{60} parent symmetry, confirming that a weak perturbation model is inadequate for these covalently bonded C_{60} balls. In particular, strongly infrared-active *T*-polymer modes with frequencies of 606 and 610 cm^{-1} are found to be derived from a linear combination of three or more I_h C_{60} parent modes. As in the *O* and *R* polymers, modes of the *T* polymer with substantial $T_{1u}(2)$ character, which are polarized in the stretched directions, are found to have large downshifts. Finally, in our comparison of theory with experiment, we find indications that the in-plane lattice of the *T* polymer may not actually be square.

DOI: 10.1103/PhysRevB.65.085413 PACS number(s): 78.30.Na, 78.30.Jw

I. INTRODUCTION

C_{60} is well known to form polymeric compounds under certain conditions. The observed polymerized C_{60} structures include a one-dimensional orthorhombic (*O*) structure, and two-dimensional tetragonal (*T*) and rhombohedral (*R*) solids.[1–11] These fullerene-based polymers are usually made under high-temperature/high-pressure (HTHP) conditions, where C_{60} is polymerized *via* 2+2 cycloaddition. Recently, the *R* polymer was reported to display ferromagnetism at 300 K.[12] Among the *O*, *T*, and *R* polymers, the *T* polymer is the most difficult to prepare and isolate.[8,9] Therefore, the material is relatively unexplored experimentally, and infrared (IR) studies on the pure *T*-polymer phase are rare.[10]

The vibrational spectrum of isolated C_{60} shows four sharp IR peaks of T_{1u} origin, as expected for a cage with icosahedral symmetry.[13] Upon polymerization, the symmetry of the C_{60} ball is reduced from I_h to D_{2h} for the *O* and *T* polymers, whereas it is reduced to D_{3d} for the *R* polymer. As a result, the vibrational properties of these HTHP polymers are very different from those of the isolated fullerene ball.[10,14] Of course, if the distortions upon polymerization are small enough, the vibrations of the polymers could still be described by weak perturbations of the vibrations of I_h C_{60} (see for example, Refs. 10 and 15). In linear chains of an *O* polymer, each C_{60} ball is distorted by two 2+2 cycloaddition polymer connections, and in the *R*-polymer planes, each C_{60} ball is distorted by six 2+2 connections. The *T* polymer is an intermediate case, the ball being distorted by four 2+2 connections. In our earlier IR study[16] of *O* and *R* polymers, we found that modes of primarily $T_{1u}(2)$ parentage, polarized in the stretched directions, are strongly downshifted to a frequency below that of any modes with substantial $T_{1u}(1)$ character. The fact that this large downshift (more than 50 cm^{-1}) occurs even for the *O* polymer, which is the least distorted of these HTHP polymers, is already an indication that the polymer-ball distortions are too large to permit the use of a weak perturbation model for the assignment of vibrations. An accurate theoretical method, such as quantum molecular dynamics (QMD), which takes into account the relaxed atomic positions in the distorted polymer balls, is thus necessary.

In this paper, we report the far-infrared vibrational properties of the *T* polymer, as an extension to our previous work on *O* and *R* materials. The IR features of the *T* polymer are assigned according to our first-principles QMD calculations. In contrast to our earlier analysis for *O* and *R* polymers, in which the I_h C_{60} parent symmetry of each polymer vibra-

tional mode was estimated by means of a visual comparison of polymer and C_{60} mode patterns, for the *T* polymer, we have determined parent symmetries quantitatively by expanding the *T*-polymer vibrational eigenvectors in terms of our calculated eigenvectors for I_h C_{60}. This analysis confirms that a weak perturbation model cannot adequately describe the vibrations of a *T* polymer. In addition, to test the possibility that the in-plane lattice of the *T* polymer might not be square, we compare the experimental results with the calculated frequencies of the *T* polymer for both square and nonsquare versions.

II. MATERIALS AND METHODS

A. Experiment

The synthesis of the *T* polymer was described in detail in Refs. 8 and 10. The tetragonal structure was confirmed by x-ray diffraction. To prepare the pellets for our measurements, the material was crushed into powder, ground with paraffin at 77 K, and compressed under vacuum at 1.5 kbar. The *T*-polymer powder was evenly suspended in the paraffin matrix to form dark brown pellets, suitable for far-infrared transmittance measurements. Several different pellet concentrations were required to reveal all features.

Far-infrared transmittance measurements were carried out on a Bruker 113V Fourier transform IR spectrometer equipped with a He-cooled Si bolometer detector. The spectral range from 30–620 cm^{-1} was covered with four different beamsplitters. The measurements were done at low temperature ($\sim$10 K), achieved with an open-flow cryostat. The spectral resolution is 0.5 cm^{-1}. It is our experience that both low temperature and high resolution are helpful to resolve weak modes and narrow line shapes. All features reported here are reproducible with different concentrations of *T* polymer in paraffin pellets.

B. Theory

Our theoretical method is quantum molecular dynamics, a first-principles technique initiated by Sankey and Niklewski.[17] QMD is based on the local density and pseudopotential approximations; details of the method were described briefly in Ref. 16, and extensively in Ref. 18. The method was applied successfully to fullerene molecules,[19] polymerized fullerenes,[16,18,20,21] and carbon solids.[22] Our calculated vibrational frequencies are known to be reliable, especially in our frequency region of interest; 200–600 cm^{-1} (Ref. 23). On the other hand, as discussed in Refs. 16, 18, and 24, our first-principles IR strengths are not fully reliable for all modes, and as a consequence we have not used them here.

The simulated structures for this work are shown in Fig. 1. In addition to the infinite *T*-polymer plane of Fig. 1(a), we also simulated three structures which contain C_{60} balls which will be present at the edges [Fig. 1(b)] and corners [Fig. 1(c)] of *T*-polymer domains. The two infinite double chains of Fig. 1(b) contain C_{60} balls which we call, left to right, ''perpendicular edge'' and ''parallel edge,'' respectively. For the perpendicular- (parallel-) edge C_{60} balls, the connecting four rings running along the double-chain direction are perpendicular (parallel) to the polymer plane. The domain-corner C_{60} balls are simulated in the infinite zigzag chain of Fig. 1(c). Note that each of the structures of Figs. 1(b) and 1(c) contains only one type of C_{60} ball.[25]

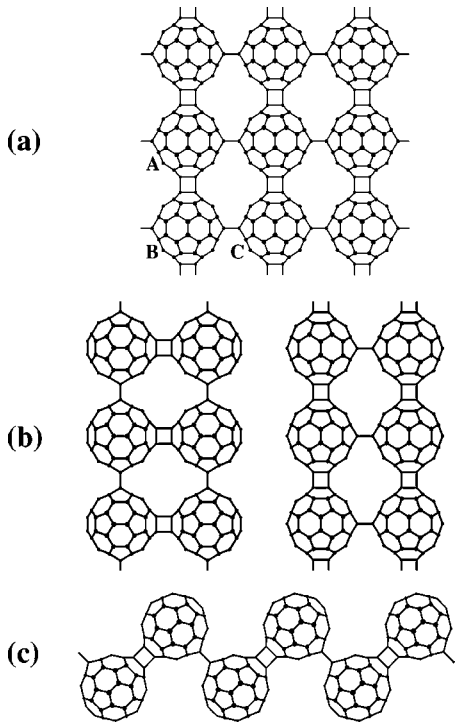

FIG. 1. Final QMD-relaxed configurations of the *T* polymer and of the three structures which contain the C_{60} balls most likely to be found at the edges and corners of finite *T*-polymer domains. (a) The nonsquare *T* polymer. (b) Left side: double chain containing perpendicular-edge C_{60} balls; the four-rings along the edge are perpendicular to the polymer plane. Right side: double chain containing parallel-edge C_{60} balls. (c) Zigzag chain with C_{60} balls having 90° angles between the two polymer connections; these are the corner balls of *T*-polymer domains. All four figures depict fragments of infinite structures.

For a *T* polymer, we find that the lowest-energy configuration is not square, but rather has two distinct center-of-mass (CM) separation distances, 9.03 Å in the chain direction having the connecting four-rings parallel to the polymer plane (*AB* in Fig. 1) and 9.13 Å in the orthogonal chain direction (*BC* in Fig. 1). We will thus refer to our lowest-energy *T*-polymer configuration as a ''nonsquare'' *T* polymer. These results for the *T* polymer confirm previous empirical-tight-binding results,[26] which found 9.06 and 9.13 Å for the CM separation distances along the *AB* and *BC* directions, respectively. These calculated differences for intermolecular distances in the tetragonal polymerized layers could easily be established by diffraction experiments if the *T* phase had the *Immm* symmetry suggested in Ref. 3. However, packing-energy calculations[27] showed that the orthorhombic *Immm* structure of the *T* phase has an energy $\sim$0.041 eV/atom higher than the $P4_2/mmc$ tetragonal layer packing. The latter model, which contains successive layers stacked along [001] via a 4_2 screw axis, i.e., neighboring layers are related

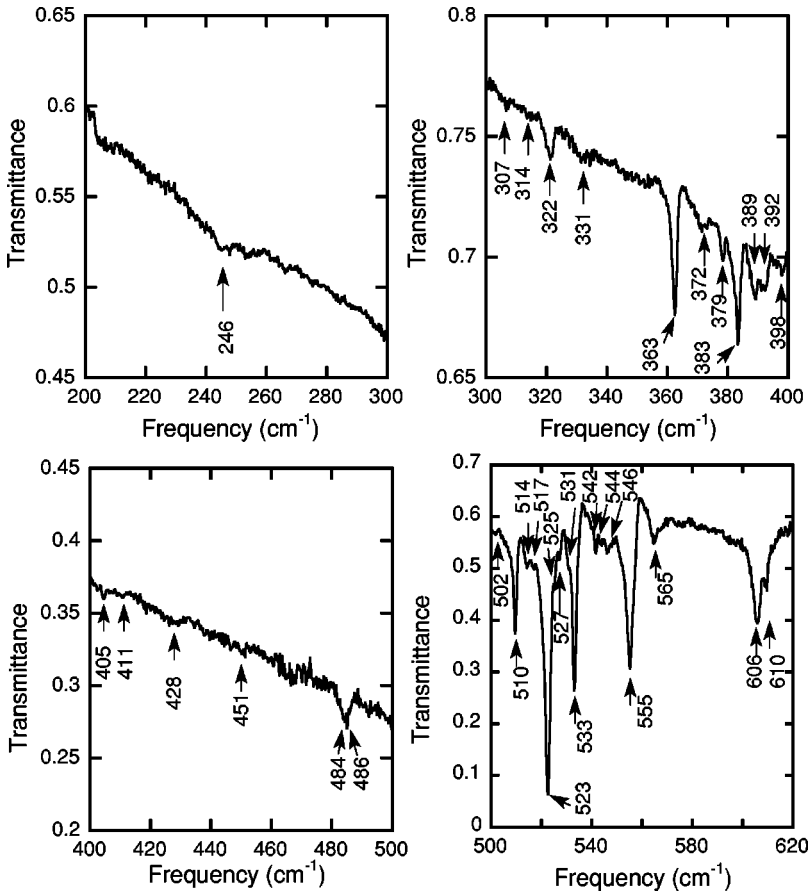

FIG. 2. 10-K transmittance spectrum of the *T* polymer. Frequencies are labeled for all reproducible modes. Different concentrations of the *T* polymer in the paraffin matrix account for variable background transmittance levels in the various panels.

by a rotation of 90°, is supported experimentally.[11] Therefore, any difference in intermolecular distances becomes undetectable in the diffraction experiments, and the *T*-phase parameters present averaged values of the intermolecular distances in the *T* layers.

We have also relaxed the *T* polymer under the constraint that the lattice vectors remain square. The resulting energy is only an insignificant 0.0003 eV/atom higher than the energy of the nonsquare configuration, so it is possible that interlayer forces might induce truly square planes. Since the x-ray-diffraction results[3,11] may be explained either by successive planes with alternating short and long directions, or by a planar structure which is actually square,[27] we will present our theoretical results for both square and nonsquare configurations. We find that the square *T* polymer has a CM separation distance of 9.09 Å, which compares well with the experimental value[28] of 9.097 Å. For the nonsquare *T* polymer, we take the average of our values in the two distinct directions, yielding 9.08 Å.

III. RESULTS AND DISCUSSION

The experimental far-infrared vibrational spectrum of the *T* polymer at 10 K is presented in Fig. 2. In our measured frequency range (30–620 cm^{-1}), no intermolecular modes are observed in the frequency region of 30–200 cm^{-1}; therefore, only the spectrum from 200 to 620 cm^{-1} is shown. We assign each peak in the measured spectrum either to a calculated IR-active *T*-polymer vibrational mode, or to an IR-active mode in one of our simulated edge balls (the corner balls turned out to be unnecessary). We make these assignments by comparing our calculated mode frequencies, which, as noted above, are expected to be reliable in this frequency range, with the experimental peak frequencies as determined from the measured spectrum of Fig. 2. However, since our *T*-polymer assignments are made on the basis of frequency and the relative spacing of symmetry-related clusters, and without the benefit of reliable calculated IR-active mode strengths, some uncertainty is unavoidable, particularly for modes which are close together in frequency. Table I presents our results, based upon a comparison with our calculated mode frequencies for the nonsquare *T* polymer. The experimental peak frequencies are in the first column, with the calculated mode frequencies appearing in columns 2 and 3 (column 2 has calculated *T*-polymer mode frequencies, and column 3 has calculated edge-ball mode frequencies). The remaining columns contain the symmetry, the calculated I_h C_{60} ''parent symmetries,'' the polarization, and the percent error for each calculated mode based upon our selected assignments. Table II presents the same information, but for the square version of the *T* polymer.

Overall, agreement with experiment is slightly better for the nonsquare *T* polymer. Based on our assignments, for the 18 IR-active *T*-polymer modes in this frequency region, the magnitude of average percent error is 2.8% for the nonsquare *T* polymer and 3.7% for the square *T* polymer. Furthermore, in no part of our measured spectrum is the average error significantly smaller for the square version. On the other hand, there are several subranges of our measured spectrum

TABLE I. Experimental far-infrared frequencies of the tetragonal (T) C_{60} polymer, compared with calculated infrared-active frequencies for the nonsquare *T* polymer and for the two edge structures of Fig. 1 as simulated by first-principles QMD. The site symmetry of the *T* polymer and of both edge structures is D_{2h}, and all modes are nondegenerate. The method of parent-symmetry determination is described in the text. For the polarizations, the *z* direction is in the polymer plane along the *AB* direction of Fig. 1, the *x* direction is in the polymer plane along the *BC* direction of Fig. 1, and the *y* direction is normal to the plane of the polymer. In some cases, more than one calculated mode is assigned to one experimental peak. In those cases, the group of calculated modes is enclosed by horizontal lines.

Frequency (cm^{-1})									
Experimental	Theoretical		Symmetry	Parent symmetries			Polarization	% Error[a]	
	T	edge						*T*	edge
246		233	edge$_{\parallel}$ B_{1u}	98.8% $H_g(1)$			*x*		−5.3
		235	edge$_{\perp}$ B_{2u}	98.0% $H_g(1)$			*y*		−4.5
		235	edge$_{\perp}$ B_{1u}	98.3% $H_g(1)$			*z*		−4.5
		236	edge$_{\parallel}$ B_{3u}	94.9% $H_g(1)$			*y*		−4.1
307		309	edge$_{\parallel}$ B_{1u}	75.4% $H_g(1)$	12.6% $H_g(2)$		*x*		+0.7
314		312	edge$_{\perp}$ B_{1u}	46.7% $H_g(1)$	37.7% $T_{3u}(1)$	10.0% $H_g(2)$	*z*		−0.6
322	313		B_{2u}	92.7% $T_{3u}(1)$			*z*	−2.8	
331	326		B_{1u}	72.9% $G_u(1)$	24.7% $T_{3u}(1)$		*x*	−1.8	
363	348		B_{3u}	97.5% $G_u(1)$			*y*	−4.1	
372		366	edge$_{\perp}$ B_{2u}	78.4% $T_{3u}(1)$	14.3% $H_u(1)$		*y*		−1.6
379	367		B_{1u}	68.6% $T_{3u}(1)$	22.4% $G_u(1)$		*x*	−3.2	
383	370		B_{3u}	85.1% $T_{3u}(1)$			*y*	−3.7	
389	373		B_{2u}	93.8% $G_u(1)$			*z*	−4.1	
392	375		B_{2u}	93.9% $H_u(1)$			*z*	−4.3	
398	380		B_{1u}	95.4% $H_u(1)$			*x*	−4.5	
405	397		B_{3u}	86.0% $H_u(1)$			*y*	−3.2	
411		400	edge$_{\parallel}$ B_{2u}	91.8% $H_g(2)$			*z*		−2.7
428		417	edge$_{\perp}$ B_{2u}	91.7% $H_g(2)$			*y*		−2.6
451		441	edge$_{\perp}$ B_{1u}	49.1% $H_g(2)$	44.5% $A_g(1)$		*z*		−2.2
		441	edge$_{\parallel}$ B_{1u}	62.7% $A_g(1)$	33.6% $H_g(2)$		*x*		−2.2
484		464	edge$_{\perp}$ B_{1u}	44.6% $G_g(1)$	27.4% $A_g(1)$	18.7% $H_g(2)$	*z*		−4.1
486		466	edge$_{\parallel}$ B_{1u}	44.8% $G_g(1)$	27.5% $H_g(2)$	15.2% $A_g(1)$	*x*		−4.1
502		495	edge$_{\parallel}$ B_{3u}	61.1% $T_{3g}(1)$	28.8% $G_g(2)$		*y*		−1.4
		498	edge$_{\perp}$ B_{2u}	62.8% $T_{3g}(1)$	24.1% $G_g(2)$		*y*		−0.8
510	499		B_{1u}	76.1% $T_{1u}(2)$	12.6% $H_u(2)$		*x*	−2.3	
	500		B_{2u}	84.1% $T_{1u}(2)$			*z*	−2.0	
514		501	edge$_{\parallel}$ B_{2u}	83.3% $T_{1u}(2)$			*z*		−2.2
517		502	edge$_{\perp}$ B_{3u}	73.4% $T_{1u}(2)$	11.7% $H_u(2)$		*x*		−2.9
523	513		B_{3u}	72.5% $H_u(2)$	24.8% $T_{1u}(1)$		*y*	−1.9	
525		515	edge$_{\parallel}$ B_{3u}	74.7% $H_u(2)$	21.1% $T_{1u}(1)$		*y*		−1.9
527		517	edge$_{\perp}$ B_{2u}	61.0% $H_u(2)$	30.3% $T_{1u}(1)$		*y*		−1.9
		517	edge$_{\parallel}$ B_{1u}	66.4% $T_{1u}(2)$	20.5% $H_u(2)$		*x*		−1.9
		518	edge$_{\perp}$ B_{1u}	63.2% $T_{1u}(2)$	16.7% $H_u(2)$	13.0% $T_{1u}(1)$	*z*		−1.7
531		520	edge$_{\parallel}$ B_{2u}	80.9% $T_{1u}(1)$	14.3% $T_{3g}(1)$		*z*		−1.3
533	527		B_{2u}	86.5% $T_{1u}(1)$			*z*	−1.1	
537		525[b]	edge$_{\parallel}$ B_{3u}	30.8% $T_{1u}(2)$	20.8% $T_{1u}(1)$	20.7% $G_g(2)$	*y*		−2.2
		527	edge$_{\parallel}$ B_{1u}	72.7% $G_g(2)$	12.3% $T_{1u}(1)$	10.1% $H_u(2)$	*x*		−1.9
539		529	edge$_{\perp}$ B_{1u}	74.2% $T_{1u}(1)$	21.2% $H_u(2)$		*z*		−1.9
542		531	edge$_{\parallel}$ B_{1u}	34.1% $T_{1u}(1)$	31.4% $H_u(2)$	21.3% $G_g(2)$	*x*		−2.0
544		534	edge$_{\perp}$ B_{3u}	63.3% $T_{1u}(1)$	16.9% $T_{3g}(1)$		*x*		−1.8
546	534		B_{3u}	65.5% $T_{1u}(2)$	18.8% $T_{1u}(1)$		*y*	−1.1	
555	541		B_{1u}	52.2% $T_{1u}(1)$	40.1% $H_u(2)$		*x*	−2.5	
565	556		B_{2u}	78.6% $H_u(2)$			*z*	−1.6	
606	585		B_{1u}	35.5% $H_u(2)$	24.7% $T_{1u}(1)$	15.5% $T_{1u}(2)$	*x*	−3.5	
610	596		B_{3u}	40.4% $T_{1u}(1)$	23.0% $T_{1u}(2)$	15.5% $H_u(2)$	*y*	−2.3	
								average −2.8	

[a]% Error = [(Theory - Expt)/Expt]*100.

[b]Parent symmetry also includes 18.2% $T_{3g}(1)$.

TABLE II. Experimental far-infrared frequencies of the tetragonal (T) C_{60} polymer, compared with calculated infrared-active frequencies for the square version of the structure as simulated by first-principles QMD. The site symmetry of the square T polymer is D_{2h}, and all modes are nondegenerate. The method of parent-symmetry determination is described in the text. The polarization directions are explained in the caption for Table I. Experimental frequencies which are not assigned here are attributed to edge effects; for these assignments, see Table I. In one case, more than one calculated mode is assigned to one experimental peak; that group of calculated modes is enclosed by horizontal lines.

Frequency (cm^{-1})							
Experimental	Theoretical	Symmetry	Parent symmetries			Polarization	% Error
246,307,314	–						
322	307	B_{2u}	86.9% $T_{3u}(1)$			z	−4.7
331	322	B_{1u}	78.5% $G_u(1)$	18.7% $T_{3u}(1)$		x	−2.7
363	343	B_{3u}	98.3% $G_u(1)$			y	−5.5
372	–						
379	353	B_{3u}	93.5% $T_{3u}(1)$			y	−6.9
383	364	B_{2u}	81.1% $G_u(1)$			z	−5.0
389	368	B_{1u}	67.8% $T_{3u}(1)$	15.1% $G_u(1)$		x	−5.4
392	374	B_{2u}	84.7% $H_u(1)$	10.3% $G_u(1)$		z	−4.6
398	382	B_{1u}	86.9% $H_u(1)$			x	−4.0
405	385	B_{3u}	97.9% $H_u(1)$			y	−4.9
411, 428, 451, 484,486,502	–						
510	499	B_{2u}	84.4% $T_{1u}(2)$			z	−2.2
	503	B_{1u}	72.8% $T_{1u}(2)$	15.0% $H_u(2)$		x	−1.4
514,517	–						
523	511	B_{3u}	72.2% $H_u(2)$	24.7% $T_{1u}(1)$		y	−2.3
525,527,531	–						
533	526	B_{2u}	84.6% $T_{1u}(1)$	10.0% $H_u(2)$		z	−1.3
537,539,542,544	–						
546	528	B_{3u}	72.8% $T_{1u}(2)$	13.8% $T_{1u}(1)$		y	−3.3
555	538	B_{1u}	56.0% $T_{1u}(1)$	35.5% $H_u(2)$		x	−3.1
565	554	B_{2u}	80.9% $H_u(2)$			z	−1.9
606	586	B_{1u}	37.2% $H_u(2)$	22.1% $T_{1u}(1)$	16.6% $T_{1u}(2)$	x	−3.3
610	589	B_{3u}	47.2% $T_{1u}(1)$	17.5% $T_{1u}(2)$	15.6% $H_u(2)$	y	−3.4
							average −3.7

for which the average error is significantly smaller for the nonsquare version. For example, assignment of the 379-, 383-, and 389-cm^{-1} experimental peaks results in average errors of −3.7% and −5.8% for the nonsquare and square structures, respectively, and thus favors the nonsquare T polymer. While the present study does not resolve the square-versus-nonsquare issue, the comparison between experimental and theoretical frequencies does slightly favor the nonsquare model. A polarized experiment on a single-crystal T-polymer sample could potentially resolve the issue.[29] In the discussion which follows, we will predominantly use our calculated results for the nonsquare T polymer. This choice does not affect our overall conclusions.

The quantitative parent symmetries in Tables I and II are obtained by expanding each calculated T-polymer or edge-ball normal-mode eigenvector as a linear combination of the complete set of QMD-calculated mode eigenvectors for I_h C_{60}. With all eigenvectors normalized, the squared expansion coefficients then give the percent contributions of each I_h C_{60} mode to each of the polymer modes.[30] In our previous study of O and R polymers,[16] we relied on a visual mode-pattern identification for the assignment of polymer-mode parent symmetries. In those cases, it was necessary to assume that each polymer mode was derived from a single I_h C_{60} parent symmetry. However, the quantitative I_h C_{60} parent symmetries of Table I reveal that it is too simplistic to assume that the IR-active T-polymer modes in this frequency region are derived from single I_h C_{60} parents. In our measured frequency region, 30–620 cm^{-1}, there are six odd-parity I_h C_{60} vibrational levels, $T_{3u}(1)$, $G_u(1)$, $H_u(1)$, $T_{1u}(1)$, $H_u(2)$, and $T_{1u}(2)$, and there are 18 IR-active T-polymer modes. Table I lists only parent-symmetry contributions of 10% or more, but we find that some of these six parent levels make contributions of greater than 1% to polymer modes with frequencies as high as 1000 cm^{-1}. Furthermore, 13 parent levels from outside this frequency range are found to make contributions of greater than 1% to these 18 polymer modes. Nevertheless, if we consider only contributions of at least 10%, we do find that the six odd-parity I_h C_{60} vibrational levels in this frequency region can be considered to produce the 18 IR-active T-polymer modes. According to our eigenvector expansions, ten of the 18 IR-

active polymer modes may reasonably be considered as singly derived, i.e., the primary parent contribution is found to be 80% or more.[31] Similarly, six of the 18 polymer modes may be considered to be derived from two I_h C_{60} parents, i.e., the sum of the primary and secondary parent contributions is 80% or more. Finally, the two polymer modes assigned to the experimental peaks at 606 and 610 cm^{-1} may be considered to be derived from three I_h C_{60} parent levels. In other words, each of these last two modes is principally a linear combination of modes from the $T_{1u}(1)$, $H_u(2)$, and $T_{1u}(2)$ parent levels.

According to our assignments, the experimental peaks with contributions from $T_{3u}(1)$ and $G_u(1)$ parents are found to be mostly singly derived, and the overall splittings of the $T_{3u}(1)$ and $G_u(1)$ contributions are about the same; $\sim$60 cm^{-1}. The $H_u(1)$-parent contributions are found in three singly derived peaks with a narrow splitting of only 13 cm^{-1}. Between 510 and 610 cm^{-1}, we find a considerable mixing of the three odd-parity I_h C_{60} parents: $T_{1u}(1)$, $H_u(2)$, and $T_{1u}(2)$. Of the nine calculated *T*-polymer modes which are assigned to experimental peaks in this frequency region, only three are found to be singly derived (all of which are polarized in the direction of the chains connected by in-plane four-rings—see Table I). $H_u(2)$ and $T_{1u}(2)$ contributions of greater than 10% appear in peaks over the entire frequency range, and $T_{1u}(1)$ contributions are found in peaks from 523 to 610 cm^{-1}. Several of the *T*-polymer assignments in this 510–610-cm^{-1} region merit extended discussion.

The experimental feature at 510 cm^{-1} has the lowest frequency of any peak which is assigned to a calculated mode with $T_{1u}(1)$, $H_u(2)$, or $T_{1u}(2)$ contributions. This 510-cm^{-1} feature is assigned to two nearly degenerate modes, with calculated frequencies of 499 and 500 cm^{-1}.[32] Both of these modes are primarily $T_{1u}(2)$-derived (see Table I), and they are polarized in the two in-plane directions in which the C_{60} balls are stretched (*AB* and *BC* in Fig. 1). In I_h C_{60}, the $T_{1u}(2)$ modes have frequencies of 575 cm^{-1}, higher than the frequencies of either the $T_{1u}(1)$ modes, at 526 cm^{-1}, or the $H_u(2)$ modes, at 534 cm^{-1}. Therefore, the major $T_{1u}(2)$ contributions polarized in the stretched directions are downshifted below any major $T_{1u}(1)$ or $H_u(2)$ contribution. This strong $T_{1u}(2)$-parent downshift is also found in the spectra of the *O* and *R* polymers,[16] and thus is a common feature of all three HTHP polymers.

The IR peak at 523 cm^{-1} is the strongest in our measured frequency range (Fig. 2), and is assigned to a calculated mode which is principally $H_u(2)$-derived [72.5% $H_u(2)$ and 24.8% $T_{1u}(1)$]. The assignment of this peak as principally $H_u(2)$-derived is somewhat surprising, since in I_h C_{60} the $T_{1u}(1)$ modes exhibit the strongest IR absorption and the $H_u(2)$ modes are not infrared active. Furthermore, the I_h C_{60} $T_{1u}(1)$ frequency is 526 cm^{-1}, closer to 523 cm^{-1} than the I_h C_{60} $H_u(2)$ frequency of 534 cm^{-1}. Without benefit of a calculation, the 523 cm^{-1} experimental feature would almost certainly have been expected to be derived principally from I_h C_{60} $T_{1u}(1)$.

On the other hand, the weak experimental peak at 546 cm^{-1} is assigned to a calculated mode which is a mixture of $T_{1u}(2)$ (65.5%) and $T_{1u}(1)$ (18.8%) parents, polarized in the normal-to-plane, or nonstretched direction. Since $T_{1u}(1)$ and $T_{1u}(2)$ are the strongest of the IR-active I_h C_{60} modes, it is interesting that a polymer mode derived from the two would be comparatively weak. For the *O* polymer, the predominantly $T_{1u}(2)$-derived modes polarized in the unstretched directions were also assigned to relatively weak experimental peaks.[16] But for the *R* polymer, the $T_{1u}(2)$-derived mode polarized in the normal-to-plane direction was best assigned to a relatively strong experimental peak.[16] A polarized experiment on a single-crystal *T*-polymer sample, or a fully reliable calculation of IR strengths, would be useful to reduce uncertainty in the 546-cm^{-1} peak assignment.

As already mentioned, the experimental peaks at 606 and 610 cm^{-1} are assigned to calculated modes which are found to be triply derived, i.e., to be linear combinations of $T_{1u}(1)$, $H_u(2)$, and $T_{1u}(2)$ parent modes. These two peaks, which are assigned to the most collective of the IR-active *T*-polymer modes in our measured frequency range, make up a prominent feature in the measured *T*-polymer spectrum, a feature which is more than 30 cm^{-1} from the nearest measured frequency of any odd-parity I_h C_{60} level [the $T_{1u}(2)$ level at 575 cm^{-1}], and which is characteristic of all three HTHP polymers. This feature occurs at 613 and 610 cm^{-1} for the *O* and *R* polymers, respectively.[16] In our previous study of the *O* and *R* polymers,[16] relying on a visual identification of mode patterns, we tentatively assigned these modes as being $H_u(2)$ derived. We have since repeated *O*- and *R*-polymer analyses with the benefit of our eigenvector expansions, and we find that, as in the case of the *T* polymer, the *O*- and *R*-polymer features at 613 and 610 cm^{-1}, respectively, should also be assigned to rather collective modes, having at least three major parent symmetry contributors in each case. The updated analysis of *R*-polymer parent symmetries, using the measured spectrum from Ref. 16, is presented in the Appendix. The reassignment of the *R*-polymer spectrum is of considerable interest in light of the recently reported 300-K ferromagnetic properties of the *R* polymer.[12] Our updated analysis of the *O* polymer was carried out with the benefit of an improved sample and will be presented elsewhere.[33]

There are several weak but reproducible experimental peaks which we have assigned to the calculated IR-active modes of the perpendicular- and parallel-edge balls of Fig. 1(b), as indicated in Table I. The loss of inversion symmetry in these edge balls means that even-parity I_h C_{60} parent modes may contribute to IR-active polymer modes. For example, the features at 246, 307, and 314 cm^{-1}, are assigned to $H_g(1)$-derived IR-active edge-ball modes. Similarly, the features between 410 and 502 cm^{-1} in the spectrum are attributed to edge-ball modes derived from $H_g(2)$, $A_g(1)$, $G_g(1)$, and $T_{3g}(1)$; however, because the density of calculated IR-active edge-ball frequencies in this region is rather large, the assignments in this region are especially tentative. In assigning the weak experimental features which are superimposed on the peaks for *T*-polymer IR-active modes,

namely, those in the frequency regions 320–410 and 510–610 cm^{-1}, we have assumed that the calculated modes which are strong according to our *T*-polymer assignments will also be strong for the edge balls. For example, the feature at 372 cm^{-1} is assigned to a perpendicular-edge mode which is primarily $T_{3u}(1)$-derived and which has a normal-to-plane polarization. The similar calculated mode for the *T* polymer is assigned to the relatively strong experimental peak at 383 cm^{-1}. The 372-cm^{-1} feature may be thought of as a ''companion'' to the strong 383 cm^{-1} experimental peak. As another example, the two weak features at 514 and 517 cm^{-1} are assigned to the parallel- and perpendicular-edge modes which are $T_{1u}(2)$ derived, and which are polarized in the most stretched directions, namely, the directions parallel to the respective edges. These may be thought of as the companion peaks to the strong experimental peak at 510 cm^{-1}. In order to assign all of the weak experimental features, we had to make only one exception to this assumption. In this case, the very weak feature at 537 cm^{-1} is attributed to either of two modes: (a) a rather collective parallel-edge mode that has the largest $T_{1u}(2)$ parent mode contribution and is polarized in the normal-to-plane direction—this is a companion peak to the 546-cm^{-1} experimental peak, which as we have already discussed, is surprisingly weak; or (b) a mode that is principally $G_g(2)$ derived.

By calculating the relative intensities of an experimental *T* polymer peak and its companion edge peaks, and by assuming that, for a particular mode, the IR absorption per ball is approximately the same independent of the type of ball, we can estimate the ratio of *T*-polymer to edge balls. We estimate a ratio of between 5 and 12 to 1, which translates to a domain size of 24–50 nm. Because the corresponding ratio of edge to corner balls, assuming smooth edges, is thus between 20 and 50 to 1, it is reasonable that we have not assigned any of the defect-induced experimental peaks to corner balls.

IV. CONCLUSION

In summary, we have measured the far-infrared vibrational spectrum of the tetragonal C_{60} polymer, and assigned the observed spectral features according to our QMD calculations. The quantitative parent symmetries of each polymer vibrational mode have been calculated by expanding the *T*-polymer eigenvectors in terms of the eigenvectors for I_h C_{60}. We find that almost half of the IR-active *T*-polymer vibrational modes in this frequency range are derived from more than one I_h C_{60} parent symmetry. In particular, in the frequency range between 500 and 620 cm^{-1}, the *T*-polymer modes tend to be collective in nature. The strong downshift of the $T_{1u}(2)$-derived modes which are polarized in the stretched directions, a downshift which had already been observed for the *O* and *R* polymers, is also found for the *T* polymer. These results are in line with the reduced symmetry and the considerable distortion of the C_{60} ball due to covalent bond formation in the *T* polymer, and confirm that a weak perturbation model is not appropriate for understanding the vibrational properties of these covalently bonded C_{60} balls. Finally, we have presented theoretical results for both square and nonsquare configurations of the *T*-polymer planes. The calculated IR-active frequencies for either version provide a satisfactory fit with experiment; however, a slightly better agreement for the nonsquare version does leave open the

TABLE III. Experimental and calculated far-infrared frequencies of the rhombohedral (*R*) polymer. The site symmetry of the *R* polymer is D_{3d}, and the infrared-active modes are twofold degenerate (E_u) or nondegenerate (A_{2u}). The method of parent-symmetry determination is described in the text.

Frequency (cm^{-1})							
Experimental	Theoretical	Symmetry	Parent symmetries			Polarization	% Error
319	299	E_u	49.9% $T_{3u}(1)$	28.2% $G_u(1)$	19.8% $H_u(1)$	in-plane	−6.3
-	320	E_u	54.3% $G_u(1)$	36.5% $T_{3u}(1)$		in-plane	−
362	336	A_{2u}	98.1% $G_u(1)$			normal-to-plane	−7.2
383	366	E_u	79.7% $H_u(1)$	10.8% $T_{3u}(1)$		in-plane	−4.4
398	401	E_u	78.4% $H_u(1)$	10.9% $G_u(1)$		in-plane	+0.8
450	429	A_{2u}	82.1% $T_{3u}(1)$			normal-to-plane	−4.7
510	491	E_u	63.6% $T_{1u}(2)$	13.6% $H_u(2)$	11.3% $T_{1u}(1)$	in-plane	−3.7
515	496	A_u	Four-connected ball, $T_{1u}(2)$			-	−3.7
522	508	A_u	Four-connected ball			-	−2.7
525	512	E_u	70.9% $H_u(2)$	9.8% $T_{1u}(1)$		in-plane	−2.5
531	523	A_{2u}	71.5% $T_{1u}(1)$	11.1% $T_{1u}(2)$		normal-to-plane	−3.5
538	530	A_u	Four-connected ball			-	−1.5
552	534	E_u	53.9% $H_u(2)$	20.0% $T_{1u}(2)$	18.1% $T_{1u}(1)$	in-plane	−3.3
557	538	A_{2u}	79.5% $T_{1u}(2)$	13.8% $T_{1u}(1)$		normal-to-plane	−3.4
567	555	A_u	Four-connected ball			-	−2.1
610	598 [a]	E_u	33.8% $T_{1u}(1)$	28.3% $H_u(2)$	18.5% $H_u(3)$	in-plane	−2.0
							average −3.3

[a]The parent symmetry also includes 11.6% $H_u(4)$.

possibility that the in-plane lattice of the *T* polymer may, in fact, be nonsquare.

ACKNOWLEDGMENTS

This work was supported by the Materials Science Division, Office of Basic Energy Sciences, U.S. Department of Energy under Grant No. DE-FG0201-ER45885 at the University of Tennessee, the Division of Materials Research at the National Science Foundation under Grant No. 9624102 at Arizona State University, the Hungarian National Science Foundation (OTKA Grant Nos. 22404 and 29931) in Budapest, and the Russian Foundation for Basic Research (Grants Nos. 00-03-32600 and IR-97-1015) at the Institute for High Pressure Physics. We thank V. C. Long and V. Agafonov for useful discussions.

APPENDIX

Table III gives the experimental and calculated far-infrared frequencies of the *R* polymer. The data are taken from our previous work,[16] and reanalyzed using the method of parent-symmetry determination detailed in Sec. III.

[1] P. W. Stephens, G. Bortel, G. Faigel, M. Tegze, A. Jánossy, S. Pekker, G. Oszlányi, and L. Forró, Nature (London) **370**, 636 (1994).

[2] Y. Iwasa, T. Arima, R. M. Fleming, T. Siegrist, O. Zhou, R. C. Haddon, L. J. Rothberg, K. B. Lyons, H. L. Carter, Jr., A. F. Hebard, R. Tycko, G. Dabbagh, J. J. Krajevski, G. A. Thomas, and T. Yagi, Science **264**, 1570 (1994).

[3] M. Núñez-Regueiro, L. Marques, J.-L. Hodeau, O. Béthoux, and M. Perroux, Phys. Rev. Lett. **74**, 278 (1995).

[4] L. Marques, J.-L. Hodeau, M. Núñez-Regueiro, and M. Perroux, Phys. Rev. B **54**, 12 633 (1996).

[5] G. Oszlányi, G. Bortel, G. Faigel, L. Gránásy, G. M. Bendele, P. W. Stephens, and L. Forró, Phys. Rev. B **54**, 11 849 (1996).

[6] R. Moret, P. Launois, P.-A. Persson, and B. Sundqvist, Europhys. Lett. **40**, 55 (1997).

[7] V. D. Blank, S. G. Buga, G. A. Dubitsky, N. R. Serebryanaya, M. Yu. Popov, and B. Sundqvist, Carbon **36**, 319 (1998).

[8] V. A. Davydov, L. S. Kashevarova, A. V. Rakhmanina, V. Agafonov, H. Allouchi, R. Céolin, A. V. Dzyabchenko, V. M. Senyavin, and H. Szwarc, Phys. Rev. B **58**, 14 786 (1998).

[9] V. A. Davydov, L. S. Kashevarova, A. V. Rakhmanina, V. Agafonov, H. Allouchi, R. Céolin, A. V. Dzyabchenko, V. M. Senyavin, H. Szwarc, T. Tanaka, and K. Komatsu, J. Phys. Chem. B **103**, 1800 (1999).

[10] V. A. Davydov, L. S. Kashevarova, A. V. Rakhmanina, V. M. Senyavin, R. Céolin, H. Szwarc, H. Allouchi, and V. Agafonov, Phys. Rev. B **61**, 11 936 (2000).

[11] R. Moret, P. Launois, T. Wågberg, and B. Sundqvist, Eur. Phys. J. B **15**, 253 (2000).

[12] T. L. Makarova, B. Sundqvist, R. Höhne, P. Esquinazi, Y. Kopelevich, P. Scharff, V. A. Davydov, L. S. Kashevarova, and A. V. Rakhmanina, Nature (London) **413**, 716 (2001).

[13] W. Krätschmer, K. Fostiropoulos, and D. R. Huffman, Chem. Phys. Lett. **170**, 167 (1990).

[14] A. M. Rao, P. C. Eklund, J.-L. Hodeau, L. Marques, and M. Núñez-Regueiro, Phys. Rev. B **55**, 4766 (1997).

[15] K. Kamarás, Y. Iwasa, and L. Forró, Phys. Rev. B **55**, 10 999 (1997); **57**, 5543(E) (1998).

[16] V. C. Long, J. L. Musfeldt, K. Kamarás, G. B. Adams, J. B. Page, Y. Iwasa, and W. E. Mayo, Phys. Rev. B **61**, 13 191 (2000).

[17] O. F. Sankey and D. J. Niklewski, Phys. Rev. B **40**, 3979 (1989).

[18] G. B. Adams and J. B. Page, in *Fullerene Polymers and Fullerene-Polymer Composites*, edited by P. C. Eklund and A. M. Rao (Springer-Verlag, Berlin, 2000), p. 185.

[19] G. B. Adams, J. B. Page, O. F. Sankey, K. Sinha, J. Menéndez, and D. R. Huffman, Phys. Rev. B **44**, 4052 (1991); G. B. Adams, O. F. Sankey, J. B. Page, M. O'Keeffe, and D. A. Drabold, Science **256**, 1792 (1992).

[20] G. B. Adams, J. B. Page, O. F. Sankey, and M. O'Keeffe, Phys. Rev. B **50**, 17 471 (1994).

[21] G. B. Adams, J. B. Page, M. O'Keeffe, and O. F. Sankey, Chem. Phys. Lett. **228**, 485 (1994); J. R. Fox, G. P. Lopinski, J. S. Lannin, G. B. Adams, J. B. Page, and J. E. Fischer, *ibid.* **249**, 195 (1996).

[22] G. B. Adams, M. O'Keeffe, O. F. Sankey, and J. B. Page, in *Novel Forms of Carbon*, edited by C. L. Renschler, J. J. Pouch, and D. M. Cox, MRS Symposia Proceedings No. 270 (Materials Research Society, Pittsburgh, 1993), p. 103; M. O'Keeffe, G. B. Adams, and O. F. Sankey, Phys. Rev. Lett. **68**, 2325 (1992); G. B. Adams, O. F. Sankey, J. B. Page, and M. O'Keeffe, Chem. Phys. **176**, 61 (1993); G. B. Adams, M. O'Keeffe, A. A. Demkov, O. F. Sankey, and Y. M. Huang, Phys. Rev. B **49**, 8048 (1994).

[23] For the 13 I_h C_{60} vibrational frequencies in the range 200 to 600 cm^{-1}, QMD yields an average percent error of 1.3%. (Ref. 24). All 13 calculated frequencies are slightly low, with the greatest errors occurring for the lowest frequencies [4.8% for I_h C_{60} $H_g(1)$ and 3.5% for I_h C_{60} $T_{3u}(1)$].

[24] J. Menéndez and J. B. Page, in *Light Scattering in Solids, VIII*, edited by M. Cardona and G. Güntherodt (Springer, Heidelberg, 2000), p. 27.

[25] For *T*-polymer simulations, we have used one C_{60} ball per periodic unit cell, resulting in all mode displacement patterns being identical on each ball. That is, all modes are of zero wave vector in a one-ball-per-cell description. For the edge and corner simulations, it is necessary to use two C_{60} balls per unit cell; however, in our frequency region of interest, above 200 cm^{-1}, all vibrational modes are intraball, i.e., the mode patterns on the two balls of the unit cell are either identical or of opposite sign. For the *T*-polymer simulation, we used four special *k* points [see H. J. Monkhorst and J. D. Pack, Phys. Rev. B **13**, 5188 (1976)] in the two-dimensional (2D) Brillouin zone, and for the chain simulations we used two special *k*-points in the 1D zone.

[26] C. H. Xu and G. E. Scuseria, Phys. Rev. Lett. **74**, 274 (1995).

[27] V. A. Davydov, V. Agafonov, A. V. Dzyabchenko, R. Céolin, and H. Szwarc, J. Solid State Chem. **141**, 164 (1998).

[28] V. M. Senyavin, V. A. Davydov, L. S. Kashevarova, A. V. Rakhmanina, V. Agafonov, H. Allouchi, R. Céolin, G. Sagon, and H. Szwarc, Chem. Phys. Lett. **313**, 421 (1999).

[29] Using the nonsquare *T*-polymer results, the 379 cm^{-1} experimental peak is assigned to in-plane polarization and the 383-cm^{-1} peak is assigned to normal-to-plane polarization. Using square *T*-polymer results, these assignments are reversed. Therefore, a polarized experiment should be able to distinguish between the two models.

[30] The *T*-polymer and edge-simulation unit cells both have D_{2h} point symmetries, which results in no symmetry-induced frequency degeneracy. However, many of the 174 vibrational modes of I_h C_{60} are degenerate; I_h C_{60} has only 46 distinct frequencies. Therefore, we sum the percent contributions from the degenerate modes within each distinct I_h C_{60} frequency level, and as a result the percentages in the parent symmetries of Tables I and II are the total percent contributions from the distinct I_h C_{60} frequency levels. A group-theoretical analysis of an I_h to D_{2h} symmetry reduction indicates that for each odd-parity I_h vibrational level, except for the nondegenerate A_u mode, there will be three IR-active D_{2h} vibrational modes. Therefore, when I_h-symmetric C_{60} balls of fcc C_{60} solid are transformed into D_{2h}-symmetric C_{60} balls of the *T* polymer, the 23 odd-parity I_h C_{60} parent levels, one of which is A_u, will result in 66 IR-active D_{2h} vibrational modes for the polymer. Thus, in our fractional parent symmetries for the *T* polymer, the total contribution of any I_h C_{60} parent level to all 66 IR-active polymer vibrational modes is 300%.

[31] By this definition, the mode assigned to the experimental peak at 565 cm^{-1} is borderline singly derived. For the square version, the parent symmetry of this mode is 80.9% $H_u(2)$, but for the nonsquare version the parent symmetry is only 78.6% $H_u(2)$ with the largest secondary contribution being 6.9% $T_{1u}(2)$. We have counted this mode as singly derived.

[32] An alternate assignment for the two calculated modes of frequencies 499 and 500 cm^{-1} would be to the experimental peaks at 510 and 514 cm^{-1}, which are dramatically different in intensity. We have chosen the accidentally degenerate assignment because we can see no likely reason, at this time, for the two calculated modes to have dramatically different intensities.

[33] Z.-T. Zhu, V. C. Long, J. L. Musfeldt, K. Kamarás, G. B. Adams, J. B. Page, V. A. Davydov, Y. Iwasa, and W. E. Mayo (unpublished).